available at www.sciencedirect.com

ScienceDirect

www.elsevier.com/locate/brainres

BRAIN RESEARCH

Research Report

Side by side comparison between dynamic versus static models of blood–brain barrier *in vitro*: A permeability study

Stefano Santaguida[a], *Damir Janigro*[a,c,d], *Mohammed Hossain*[a], *Emily Oby*[a], *Edward Rapp*[b], *Luca Cucullo*[a,*]

[a]*Division of Cerebrovascular Research, Cleveland Clinic Lerner College of Medicine, Cleveland, OH 44106, USA*
[b]*Clevemed, Cleveland Clinic Lerner College of Medicine, Cleveland, OH 44106, USA*
[c]*Department of Neurosurgery, Cleveland Clinic Lerner College of Medicine, Cleveland, OH 44106, USA*
[d]*Department of Molecular Medicine, Cleveland Clinic Lerner College of Medicine, Cleveland, OH 44106, USA*

ARTICLE INFO

Article history:
Accepted 11 June 2006
Available online 20 July 2006

Keywords:
Drug delivery
Gene therapy
Cerebral blood flow
Shear stress
Glia–vascular interaction

ABSTRACT

Endothelial cells *in vivo* are continuously exposed to shear stress, a tangential force generated by the flow of blood across their apical surfaces that affects endothelial cell structure and function. By contrast, the Transwell apparatus cannot reproduce the presence of intraluminal blood flow that is essential for the formation and differentiation of the BBB. In contrast, the dynamic *in vitro* model of the BBB (DIV-BBB) mimics both functionally and anatomically the brain microvasculature, creating quasi-physiological conditions for co-culturing human and non-human endothelial cells and astrocytes in a capillary-like structure. We used intraluminal bovine aortic endothelial cells (BAEC) co-cultured with extraluminal glial cells (C6) to obtain elevated trans-endothelial electrical resistance (TEER) and selective permeability to sucrose and phenytoin. The experiments were performed in parallel using Transwell systems DIV-BBB models and data were then cross compared. By contrast with Transwell, C6 and BAEC co-cultured in the DIV-BBB demonstrated predominantly aerobic metabolism evidenced by a robust increase in glucose consumption that was paralleled by a similar change in lactate production. BAEC exposed to glia under dynamic conditions grow in a monolayer fashion and developed a more stringent barrier as demonstrated by high TEER values and a selective permeability to [^{14}C] phenytoin and the well-known paracellular marker [^{3}H] sucrose. In conclusion, these data demonstrate that the exposure to intraluminal flow plays an essential role in promoting endothelial cell differentiation and increasing BBB tightness, thus making the use of the DIV-BBB well suited for pharmacological studies.

1. Introduction

The BBB is found in the brain of all vertebrates (Abbott, 2005). Morphologically, the BBB is formed by specialized endothelial cells (ECs) paving the luminal side of brain microvessels in close association with abluminal astrocytic end-feet processes sharing the basal lamina and enveloping more than 98% of the BBB endothelium (Emmi et al., 2000). Astrocytes interact with the

* *Corresponding author*. Project Scientist, Cleveland Clinic Foundation NB20, Neurosurgery, 9500 Euclid Avenue/NB20, Cleveland, OH 44195, USA. Fax: +1 216 444 1466.
E-mail address: cuculll@ccf.org (L. Cucullo).

0006-8993/$ – see front matter © 2006 Elsevier B.V. All rights reserved.
doi:10.1016/j.brainres.2006.06.027

cerebral endothelium to determine BBB function; they also regulate protein expression, modulate endothelium differentiation, and appear to be critical for the induction and maintenance of the tight junctions and BBB properties (Abbott, 2005; Liberto et al., 2004; Stanness et al., 1997; Mizuguchi et al., 1997; Hamm et al., 2004; Hori et al., 2004; Kramer et al., 2002). The microvascular endothelium at the BBB is characterized by the presence of tight junctions (zonulae occludentes), lack of fenestrations, and minimal pinocytotic vesicles. These distinct morphological properties of the BBB account for the "restraining" nature of brain capillary ECs. In particular, tight junctions between the cerebral endothelial cells form a diffusion barrier, which selectively excludes most blood-borne substances and xenobiotics from entering the brain, protecting it from systemic influences. The transit across the BBB involves translocation through the capillary endothelium by carrier-mediated transport systems, except for lipid soluble substances such as alcohol, narcotics, and anticonvulsants that pass with ease through the endothelium layer. The BBB also provides specialized transport systems for nutrients and other biologically important substances (i.e., D-glucose, lactate, phenylalanine, choline, adenosine, arginine, adenine) (De Boer et al., 1998) from the peripheral circulation to neurons in the parenchyma. Because of its selectivity, the BBB plays a crucial role in regulating the trafficking

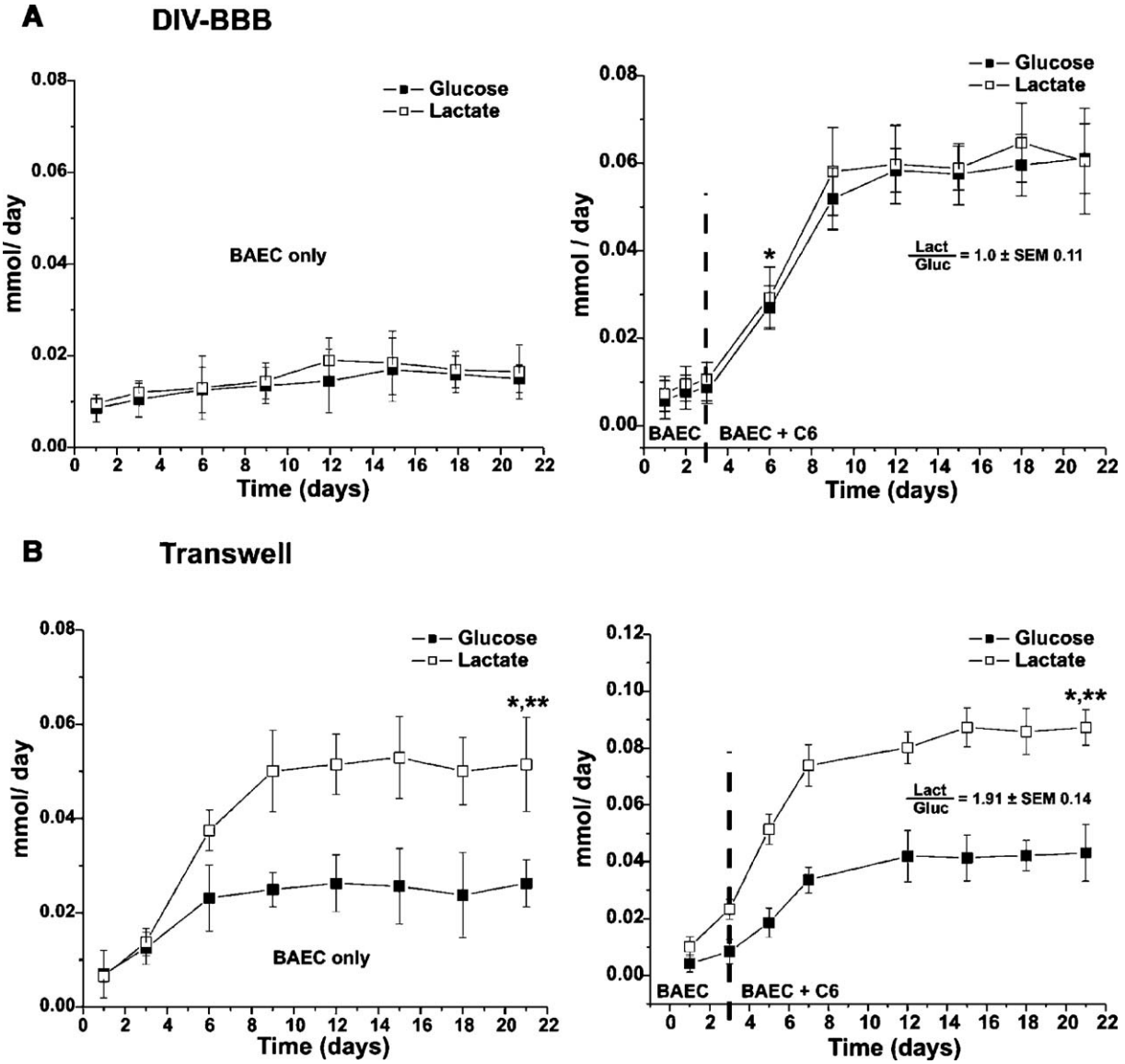

Fig. 1 – Differential metabolic pattern between BAEC cultured alone or co-cultured with C6 in DIV-BBB and Transwell. Panel A, left: metabolic pathway of monoculture of BAEC in DIV-BBB. Panel A, right: sharp metabolic increase in glucose consumption (mmol/day) paralleled by a similar increase in lactate production, thus suggesting that in DIV-BBB systems cell metabolism is principally aerobic (ratio between lactate production and glucose consumption is ≈1). By contrast, Panel B in Transwell the ratio between lactate production and glucose consumption is ≈2, thus demonstrating a different metabolic pathway (anaerobic) for cells cultured under static condition in comparison to flow-based co-cultures. Note that "*" refers to a statistically significant metabolic increase ($P<0.05$) whereas "" refers to a statistically significant ($P<0.05$) difference between glucose consumption and lactate production.**

between blood and CNS (Hagenbuch et al., 2002) and the determination of neuroimmunology and neuropathology (Banks, 2005).

BBB dysfunction has been observed in the majority of neurological diseases, but the causes of aberrant vascular behavior are generally unknown. Genomic and proteomic analyses are currently being used to examine BBB function in healthy and diseased brain to better characterize this dynamic interface (Shusta, 2005). For example, BBB permeability changes are involved in brain edema formation and central nervous system injuries, such as stroke (Heo et al., 2005), cerebral hypoxia-reoxygenation (Brown and Davis, 2005), head injuries (Korn et al., 2005), neurodegenerative diseases, and neurological infections including bacterial and viral meningitis, encephalitis, or HIV-1 infection (Toborek et al., 2005; Hawkins and Davis, 2005). How these permeability changes affect drug passage into the CNS is largely unknown. For example, because most CNS drugs are lipophilic, how perivascular edema or general BBB failure affects drug permeability is still poorly understood.

In vitro studies on reconstituted BBB models help to reveal the direct effects of pathological conditions on cerebral endothelium (Krizanac-Bengez et al., 2004), but due to sometimes high "resting" permeability values, the effects of pathogenetic factors on the impairment of barrier integrity may be obscured. CNS drug design (e.g., antineoplastics, antivirals, and antiepileptics) cannot rely entirely upon physicochemical properties to cross the BBB and remains largely studied *in vivo*. For example, lipophilicity alone is a poor predictor for drug penetration into the CNS because it relies on a passive, diffusional uptake. Many lipophylic drugs are potential substrates for efflux carriers of the BBB (particularly P-glycoprotein), which can drastically reduce their penetration into the brain (Abbott, 2002). Investigations performed on reliable *in vitro* models of BBB can be a suitable tool for testing efficacy and brain penetration of new drugs (Cucullo et al., 2002, 2005).

The aims of the present work were (1) to address some of the weaknesses of existing flow-based tissue culture apparatus (Cucullo et al., 2005); and (2) to cross compare the consistency and accuracy of drug permeability measurements in the dynamic *in vitro* BBB (DIV-BBB) model to a conventional Transwell system. For this purpose, we used a cell combination (C6 glioma and bovine aortic endothelial cells, BAEC) that has been previously shown to replicate most of the features of the blood–brain barrier relevant to our studies (Stanness et al., 1996, 1997, 1999; Cucullo et al., 2002; Pekny et al., 1998).

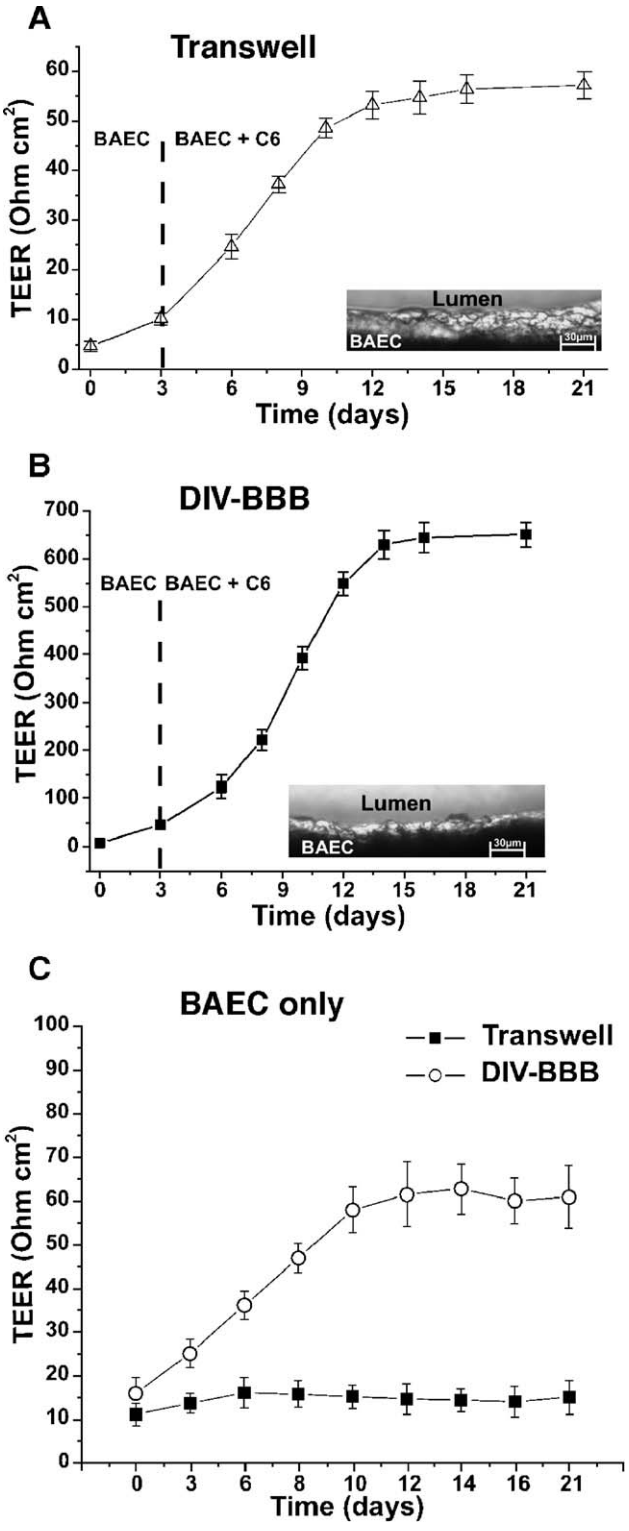

Fig. 2 – Dynamically grown endothelial cells develop higher trans-endothelial electrical resistance in comparison to Transwell. Bovine aortic endothelial cells developed a much more stringent barrier in the presence of glial cells. This is demonstrated by the rapid TEER increase in both Transwell (Panel A) and DIV-BBB apparatus (Panel B) and by the overall TEER values obtained when monoculture of BAEC are used instead (Panel C). Note, however, that under dynamic conditions, BAEC shows a more robust differentiation resulting in the development of a more stringent barrier as demonstrated by higher TEER values in comparison to Transwell. This is also evident from Panel C when BAEC are cultured without C6. The insets show parts of the cross-section of porous membranes with cells growing (section thickness 20 μm), Panel A from a Transwell membrane and Panel B from a hollow fiber of the DIV-BBB. Note that BAEC exposed to luminal flow develops in monolayer fashion inside the artificial capillary (n=19). By contrast, in Transwell system endothelial cells develop in multilayer fashion (n=12).

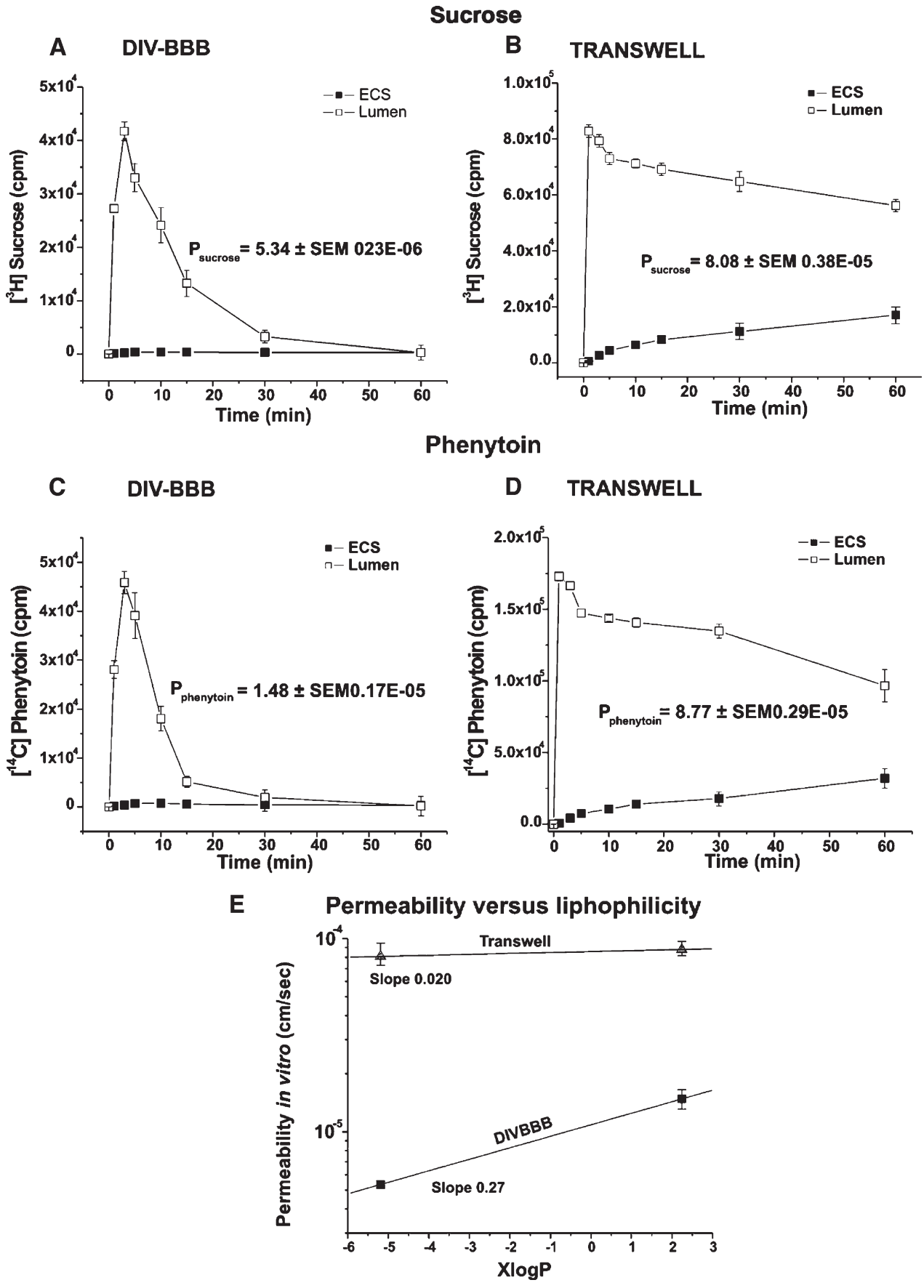
Sucrose
A
DIV-BBB
ECS
Lumen
[3H] Sucrose (cpm)
Time (min)
P sucrose = 5.34 ± SEM 023E-06
B
TRANSWELL
ECS
Lumen
[3H] Sucrose (cpm)
Time (min)
P sucrose = 8.08 ± SEM 0.38E-05
Phenytoin
C
DIV-BBB
ECS
Lumen
[14C] Phenytoin (cpm)
Time (min)
P phenytoin = 1.48 ± SEM0.17E-05
D
TRANSWELL
ECS
Lumen
[14C] Phenytoin (cpm)
Time (min)
P phenytoin = 8.77 ± SEM0.29E-05
E
Permeability versus liphophilicity
Transwell
Slope 0.020
DIVBBB
Slope 0.27
Permeability in vitro (cm/sec)
XlogP

2. Results

2.1. Cell viability and BBB integrity

Monitoring of cell metabolism is a critical step in assessing the viability of dynamically grown endothelial cells or glia (Stanness et al., 1996, 1997). Fig. 1A shows early changes in glucose consumption and lactate production in bovine aortic endothelial cells grown alone (left panel) or in co-culture with C6 glioma cells in DIV-BBB (right panel). Note that in the DIV-BBB, the glucose consumption is always paralleled by a similar lactate production indicating predominance of aerobic metabolism (lactate production–glucose consumption ratio = 1 ± SEM 0.08). The addition of glial cells to the extraluminal compartment (ECS) caused a similar robust increase in both glucose and lactate production. By contrast, in the Transwell apparatus (Fig. 1B), BAEC alone (left panel) or co-cultured with glial cells (right panel) display a lactate production–glucose consumption ratio of 1.91 ± SEM 0.14, thus suggesting that in the absence of flow the metabolism is predominantly anaerobic (Desai et al., 2002).

Peripheral endothelial cells develop negligible barrier properties in both DIV-BBB and Transwell when cultured alone (Stanness et al., 1997). However, a few days following exposure to glial cells grown extraluminally and parallel to metabolic changes, trans-endothelial electrical resistance increased dramatically in both models. Transwell achieved a stable electrical resistance of 57.2 Ω cm^2 ± SEM 2.8 (Fig. 2A). By comparison, endothelial cells exposed to glia in the presence of intraluminal flow, as in the DIV-BBB (Fig. 2B), developed a high stable TEER (650.7 Ω cm^2 ± SEM 26.5). This demonstrates that the presence of intraluminal flow is critical for the differentiation of endothelial cells and the development of functional BBB properties *in vivo*, such us high TEER. Note that despite the lack of glial cells, BAEC exhibit proportionally a much higher TEER when cultured under dynamic condition (Fig. 2C). The inserts in Fig. 2 show a cross section of a Transwell and a typical hollow fiber. Note that in contrast to the Transwell apparatus (insert in Fig. 2A), endothelial cells grown under dynamic conditions (insert if Fig. 2B) develop in a monolayer fashion, thus mimicking the structural physiology of capillaries *in vivo*.

2.2. Permeability experiment

The measurement of TEER across the endothelial cell monolayer is indicative of barrier integrity, as previously reported (Cucullo et al., 2002, 2005; Krizanac-Bengez et al., 2006). In addition, assessment of the barrier function was carried out by permeability measurements of selected molecules: phenytoin (a common antiepileptic drug) and sucrose (an established paracellular marker). A bolus containing [^{14}C] phenytoin and [^{3}H] sucrose was directly added to the medium contained in the lumen in DIV-BBB and Transwell systems. Samples were taken from both lumen and ECS over 60 min; [^{14}C] phenytoin and [^{3}H] sucrose flux were monitored by detection of the radioactive tracers. The permeability was calculated by graphical integration of the concentration of the tracer in the lumen and in the ECS.

These molecules were chosen as paracellular markers for their inability to cross cell membranes. The permeability across the endothelium in the DIV-BBB was 5.34 ± SEM 0.23×10^{-6} cm/s for [^{3}H]sucrose (Fig. 3A) and 1.48 ± SEM 0.17×10^{-5} cm/s for [^{14}C] phenytoin (Fig. 3C) calculated from the initial (60 min) time period of the time-transport profiles. In comparison, *in vitro* BBB established in the Transwell apparatus developed a less tight barrier as shown in Figs. 3B and D (permeability to sucrose was 8.08 ± SEM 0.38×10^{-5} cm/s and 8.77 ± SEM 0.29×10^{-5} cm/s for phenytoin). Note also (Fig. 3E) that the DIV-BBB can discriminate between these substances based on their permeability and oil/water partition coefficients, whereas this would be difficult to achieve in Transwell.

2.3. BBB integrity and permeability

Clinically, intracarotid infusion of hyperosmolar solutions of mannitol (1.6 M) is used to cause temporary disruption of the BBB (Hawkins and Egleton, 2006; Siegal et al., 2000; Brown et al., 2004; Rapoport, 2000; Fortin et al., 2004), thus enhancing chemotherapeutic drug penetration of the BBB in patients with malignant brain tumors or metastases (van Vulpen et al., 2002). Osmotic opening of the BBB by mannitol solution is mediated by cerebrovascular dilatation, dehydration of endothelial cells, and contraction of their cytoskeleton combining widening of the interendothelial tight junctions. This mechanism is driven solely by the effect of the osmotic impact without participation of other energy-dependent mechanisms of BBB permeability enhancement (Rapoport, 2000). We tested the effect of hyperosmolar mannitol injection on BBB permeability and integrity in a DIV-BBB. This technique was used to demonstrate that TEER and drug permeability of [^{3}H] sucrose and [^{14}C] phenytoin were principally dependent on the tightness of the established *in vitro* BBB and not related to the intrinsic resistance of the hollow fibers in the DIV-BBB or the Transwell membrane. The permeability across the *in vitro* BBB under these conditions was 2.53 ± SEM 0.22×10^{-3} cm/s and 1.48 ± SEM 0.31×10^{-3} for [^{3}H] sucrose in DIV-BBB and Transwell, respectively (Fig. 4A). In absence of a functional barrier (in consequence of the osmoting opening),

Fig. 3 – Sucrose and phenytoin permeability in DIV-BBB versus Transwell; a side-by-side comparison. Panels A and C show plots of counts per minute (cpm) vs. time from which permeability to [^{3}H] sucrose (5.34 ± SEM 0.23×10^{-6} cm/s) and [^{14}C] phenytoin (1.48 ± SEM 0.17×10^{-5} cm/s) in DIV-BBB was calculated. By contrast, *in vitro* BBB established in Transwell (as shown in Panels B and D) developed less stringent barriers resulting in higher permeability values ([^{3}H] sucrose was 8.08 ± SEM 0.38×10^{-5} cm/s whereas [^{14}C] phenytoin was 8.77 ± SEM 0.29×10^{-5} cm/s for phenytoin). Note that permeability in vivo of sucrose and phenytoin is 1×10^{-7} and 1.08×10^{-5} cm/s, respectively. Panel E shows the correlation between permeability *in vitro* and the oil/water partition coefficient (XlogP) of sucrose and phenytoin in DIV-BBB and Transwell. Note that whereas the DIV-BBB can easily discriminate between these two substances based on their lipophilicity, this will be very difficult to achieve in a Transwell.

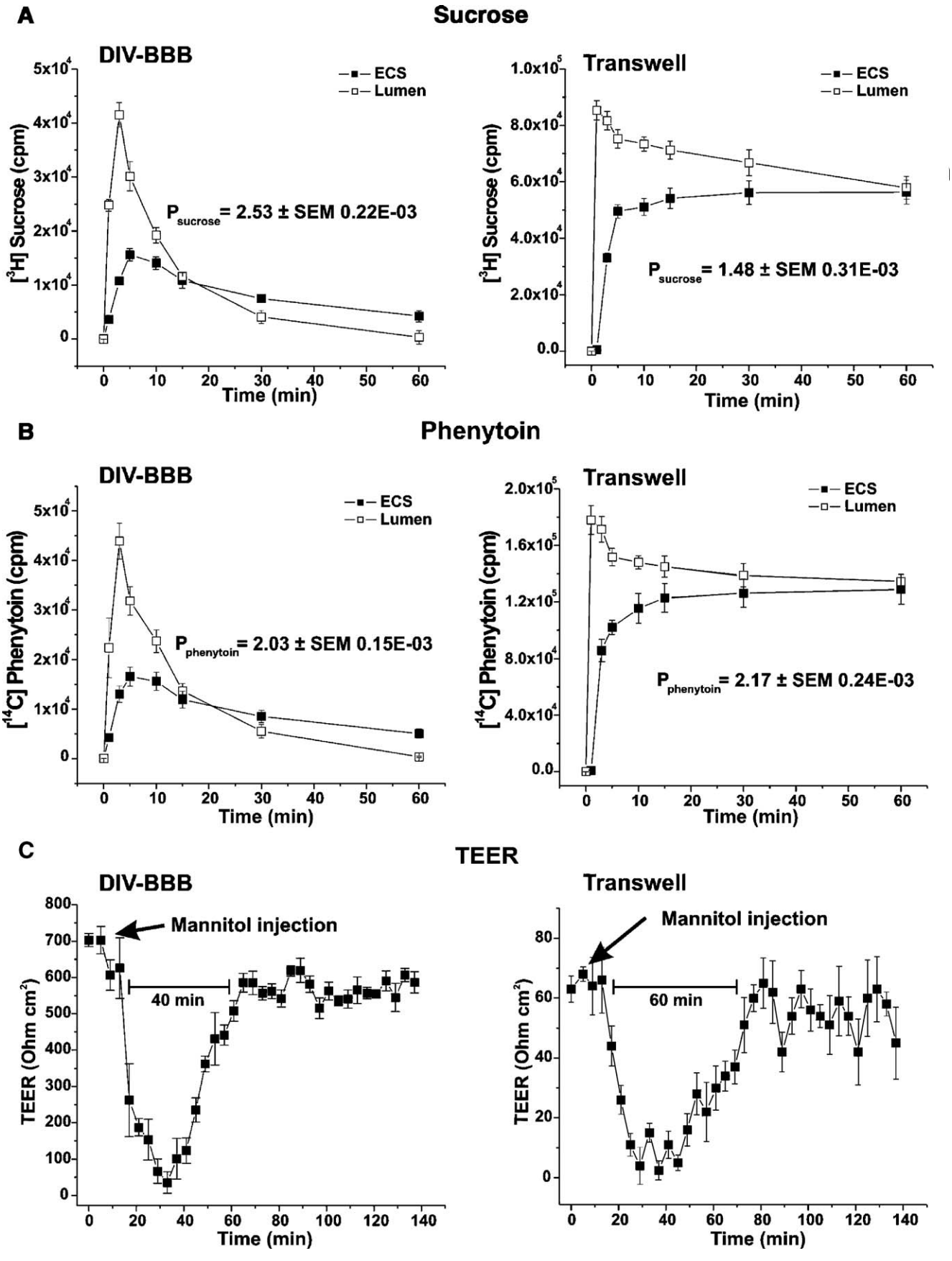
A
Sucrose
DIV-BBB
ECS
Lumen
[3H] Sucrose (cpm)
P sucrose = 2.53 ± SEM 0.22E-03
Time (min)
Transwell
ECS
Lumen
[3H] Sucrose (cpm)
P sucrose = 1.48 ± SEM 0.31E-03
Time (min)
B
Phenytoin
DIV-BBB
ECS
Lumen
[14C] Phenytoin (cpm)
P phenytoin = 2.03 ± SEM 0.15E-03
Time (min)
Transwell
ECS
Lumen
[14C] Phenytoin (cpm)
P phenytoin = 2.17 ± SEM 0.24E-03
Time (min)
C
TEER
DIV-BBB
Mannitol injection
40 min
TEER (Ohm cm2)
Time (min)
Transwell
Mannitol injection
60 min
TEER (Ohm cm2)
Time (min)

[^{14}C] phenytoin permeability was 2.03 ± SEM 0.15 × 10^{-3} cm/s in DIV-BBB and 2.17 ± SEM 0.24 × 10^{-3} cm/s in Transwell (Fig. 4B). The permeability was calculated as previously described from the initial (60 min) period of the time-transport profiles. Note how both system reach the equilibrium between the luminal and abluminal compartment. Loss of BBB integrity was monitored by real-time TEER measuring (Fig. 4C).

3. Discussion

The BBB is a dynamic interface between the blood and the central nervous system (CNS) that controls the rate of influx and efflux of biological substances needed for the brain metabolic processes and neuronal function. The BBB phenotype develops under the influence of associated brain cells, especially astrocytes. This leads to the formation of a much more stringent tight junction system (Abbott, 2005) in comparison to other capillary endothelia. A number of specific transport and enzyme systems that regulate molecular traffic between the blood and the CNS comprise another particular characteristic of the BBB endothelium (Abbott, 2002). The barrier is additionally comprised of the basal lamina, which is an extension of the extracellular matrix (ECM). EC and astrocyte adhesion to the matrix are mediated by integrin receptors (Ellison et al., 1999).

The use of cultured vascular endothelial cells as a model of vascular permeability has significantly advanced the understanding of microvascular physiology. However, serious limitations associated with the use of cultured brain endothelial cells have hampered the development of a reliable model of the BBB. For example, it has been difficult to reproduce in cultured cells the high electrical resistance normally found across BBB endothelial cells *in situ*. Furthermore, cultured brain endothelial cells lose some of their specific markers following prolonged *in vitro* culturing (Ballermann and Ott, 1995). One approach used to mimic the growth environment of *in vivo* brain EC has been the use of glia/endothelial co-cultures (Abbott, 2002; Boveri et al., 2005; Sobue et al., 1999; Laterra and Goldstein, 1991; Minakawa et al., 1991). Alternatively, investigators have attempted to imitate the physiological environment of microvascular endothelial cells by exposing the cells to flow (Ballermann and Ott, 1995; Ballermann et al., 1998). More recent attempts have led to dynamic *in vitro* BBB models that recapitulate all these approaches (Stanness et al., 1996, 1997, 1999; Cucullo et al., 2002, 2005; Ballermann and Ott, 1995; Deli et al., 2005; Grant et al., 1998; Janigro et al., 1999; Salvetti et al., 2002).

Studies from this and other laboratories have convincingly demonstrated that the use of static models to mimic the physiological and structural characteristic of *in vivo* BBB is flawed. There are several *in vitro* models of the BBB currently employed to explore the permeability and potential efficacy of drugs targeting the brain. The most commonly used system for EC culturing consists of a porous membrane support submerged in feeding medium (e.g., Transwell apparatus). The bi-dimensional Transwell system is characterized by a side-by-side diffusion system. A major disadvantage of this system is the lack of physiologic shear stress due to the absence of intraluminal flow. The role played by intraluminal shear stress in brain microvessel endothelial cell differentiation, as well as maintenance and induction of a BBB phenotype, is now well recognized (Desai et al., 2002; Ballermann and Ott, 1995; Krizanac-Bengez et al., 2003; Brooks et al., 2004; Wasserman and Topper, 2004; Ott and Ballermann, 1995; Ando and Kamiya, 1996; Lin et al., 2000; McAllister et al., 2001).

The tightness of the barrier in Transwell, measured by both TEER and permeability to polar molecules, is typically much less stringent than the BBB *in vivo*. Thus, compounds that poorly penetrate across the BBB *in vivo* (e.g., sucrose) readily diffuse across the endothelial monolayer in the static model we examined in this study ($P_{sucrose} \approx 8.08 \times 10^{-5}$, permeability in Transwell was between 10^{-4} and 10^{-5} cm/s whereas *in vivo* it was $\approx 10^{-7}$ cm/s; see Fig. 3). Because of an elevated $P_{sucrose}$, BBB permeability, values of other compounds may be overestimated. However, the permeability values of sucrose that we measured in Transwell was higher in comparison to similar systems where instead of BAEC, porcine brain microvessel endothelial cells (PBMEC/C1-2) were used ($P_{sucrose} \approx 5 \times 10^{-5}$) (Lauer et al., 2004). Nevertheless, permeability values of sucrose measured in DIV-BBB ($P_{sucrose} \approx 5 \times 10^{-6}$) were more physiological than those reported in this more "efficient" Transwell model.

Lack of physiological conditions, such as presence of intraluminal flow, may accelerate the dedifferentiating process that the endothelial cells experience and further enhance the loss of the BBB characteristics with serial cell passage (Akimoto et al., 2000). Furthermore, increased cell cycle rate due to lack of antimitotic influences by laminin and flow will cause endothelial cells to pile up in a multilayer fashion (Ziegler and Nerem, 1994). In addition, the occurrence of irregular patterns of cell adhesion or "edge effect" in Transwell systems can seriously hamper the measurement of BBB permeability.

The DIV-BBB originates from a modification of a cell culture system used for hybridoma cell expansion. This *in vitro* "cell differentiation factory" provides quasi-physiological experimental conditions for culturing endothelial cells and astrocytes in a capillary-like structure and is able to functionally and anatomically mimic the brain microvasculature. In the hollow fiber apparatus, endothelial cells develop a morphology that closely resembles the endothelial phenotype *in situ*, demonstrating that endothelial cells grown with flow are more differentiated than after conventional culture (Stanness et al., 1997, 1999; Cucullo et al., 2002; Grant et al., 1998; Janigro et al., 1999; Salvetti et al., 2002).

Fig. 4 – Hyperosmolar opening of the BBB in DIV-BBB and Transwell models. Panels A and B show the effect of hyperosmolar mannitol on BBB permeability to sucrose and phenytoin in DIV-BBB and Transwell. Note that in absence of a functional barrier, the permeability values of [^{3}H] sucrose and [^{14}C] phenytoin) in both DIV-BBB and Transwell are similar and overall much higher then previous values measured in intact BBB. Note also that the DIV-BBB remains temporarily permeable for approximately 40 min following mannitol perfusion while this time window is approximately 60 min for Transwell.

The DIV-BBB also enables real-time continuous monitoring of BBB function by measurement of TEER across the barrier via electrodes inserted in the luminal and abluminal (ECS) compartments. Another advantage is that the exposure to a controlled pumping rates makes the model suited for the study of endothelial cell responses to a wide range of shear stress: from the one expected in brain capillaries as in the present study (~4 dyn/cm^2) to larger vessels (up to ~70 dyn/cm^2). Note, however, that as implemented today the system does not allow for the study of the effects of turbulent or otherwise altered flow. The pulsatile flow generated consists of a complex waveform with a substantial drop of pressure occurring at the end of the capillaries giving these models the ability to reproduce the hemodynamic conditions observed *in vivo* (Cucullo et al., 2002).

The need for novel pharmaceutical strategies as well as the necessity to limit the increasing costs of experimental studies, pre-screening and testing is continuously pushing researchers to develop improved *in vitro* models to accelerate drug design. For this reason, we developed an improved DIV-BBB modified to provide higher predictability and reproducibility while being fully scalable, customizable, and well suited for basic research as well as extensive or industrial use. For example, the DIV-BBBs are built with more constrained dimensions in order to minimize the number of cells necessary to set up the system as well as reducing the operating costs. This model allows on-line computer controlled TEER monitoring for a more detailed BBB integrity assessment. The electrodes are built into the cartridge to reduce risk of external contamination (Fig. 5). Experimental data have shown that using a co-culture of BAEC and C6 our model can yield TEER values ≈700 Ω cm^2 (see Fig. 1) that more closely resemble physiological resistance *in vivo*. Permeability to sucrose (5.34 ± SEM 0.23 × 10^{-6} cm/s) and phenytoin (1.48 ± SEM 0.17 × 10^{-}5 cm/s) are also in agreement with data *in vivo* (1 × 10^{-7} and 1.08 × 10^{-5} cm/s, respectively). Several DIV-BBBs can be multiplexed (stackable units) yet remain independent of one another and BBB integrity can be assessed by TEER monitoring in the same way. This is extremely important when different experimental paradigms need to be tested. The correlation established between the TEER measurements and drug permeability during the BBB opening after exposure to hyperosmolar mannitol (see Fig. 4C) demonstrates the reliability and accuracy of this method to assess for BBB integrity without having to perform time consuming permeability experiments with paracellular markers. The DIV-BBB retains the BBB properties for several months under sterile and appropriate culture conditions (Stanness et al., 1996, 1997).

In conclusion, we have described the properties of a novel tissue co-culture apparatus that enables endothelial differentiation under controlled conditions that closely mimic the BBB *in situ*. Both permeability to polar molecules and TEER were compared with parallel glia–endothelial cells static co-cultures established in Transwell apparatus, demonstrating that the lack of physiological conditions in Transwell hamper BBB functionality and selective permeability. DIV-BBB advantages are summarized in Table 1. Future versions of our model will generate a fully automated flow-based *in vitro* BBB. We also expect that by using co-cultures of human brain microvascular endothelial cells (HBMEC) and human astrocytes we will be able to achieve even tighter *in vitro* BBB with physiological and functional characteristic similar to the BBB *in vivo*. Microdialysis probes (customized for a variety of needs with different cutoffs) can be inserted into the capillary bundles and attached to a fraction collector, which is also computer controlled and fully programmable. Then analysis can be conducted with the glucose/lactate analyzer, HPLC, MALDI -TOF, or other devices depending on the user's criteria and purposes. Other apparatus can be designed around the DIV-BBB such as an external "turret shape" micro-incubator system that can be used to maintain the cartridges at the desired temperature avoiding the problem of manipulating the cartridges in restrained spaces (classical incubator) and to automatically control/adjust oxygen and CO_2 levels in the culture medium. The system can be fully automated, thus minimizing operator efforts. Further advancement in this field may come with the introduction of new materials or more sophisticated techniques for the manufacture of capillary-like hollow fibers, where anchoring molecules for cell adhesion can be implemented in their matrix construction, thus allowing the possibility to manufacture novel BBB models that more closely mimic the BBB *in situ*.

4. Experimental procedures

4.1. *Cell culture*

We used bovine aortic endothelial cells (BAEC) cultured alone or co-cultured with rat glioma C6 cell line. Both cell types where purchased from American Type Culture Collection (ATCC, Rockville, Maryland). Co-cultures of BAEC and C6 have been previously shown to replicate most of the features of the blood–brain barrier relevant to our studies (Stanness et al., 1996, 1997, 1999; Cucullo et al., 2002; Pekny et al., 1998; Janigro et al., 1999). Monocultures of BAEC in DIV-BBB and in Transwell where used to assess metabolic and functional changes in comparison to the BAEC–C6 co-cultures.

Cells (passages 1–5 for both BAEC and C6) were initially cultured in 75 cm^2 flasks at 37 °C in a humidified atmosphere of 5% CO_2 and expanded in Dulbecco's modified Eagle medium (DMEM-F12) with 25 mM HEPES buffer, supplemented with L-glutamine, 10% fetal bovine serum (FBS), and 100 U/mL penicillin + 100 μg/mL streptomycin (1% PEST). Culture medium was changed two times a week. Upon passage, adherent cells were washed twice with 10 mL PBS (pH 7.2) and detached with 3–5 mL trypsin for 3–5 min at 37 °C. Finally, cells were centrifuged in culture medium (200 g for 10 min) and the pellet was resuspended in culture medium at the appropriate concentration prior to seeding in the DIV-BBB system or Transwell apparatus.

4.2. *DIV-BBB setup*

The DIV-BBB model used for the experiments described herein (Fig. 5A) consists of 19 hollow polypropylene fibers (Hydrophobic capillaries Accurel® PP Q3/2; lumen total volume = 0.202 cm^3, luminal surface area = 0.71 cm^2) with a nominal

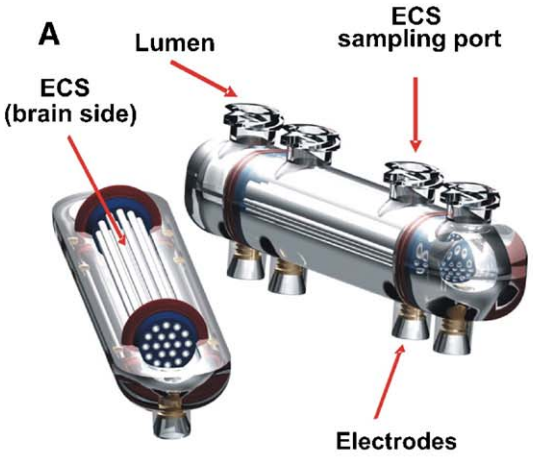

New DIV BBB

- Dimensions – 63mm x 9mm x 9mm
- Capillary number – 19
- Capillary length – 3.8 cm
- Pore size – 0.64μm
- Wall thickness – 200 μm
- Inner diameter -- 600 μm
- Diameter – 1mm
- Capillary surface area – 22.6 cm^2
- Lumen surface area – 13.5 cm^2
- ECS (functional) volume – 1.15 mL
- Single fiber volume – 0.0106 mL
- Lumen (functional) volume – 0.202 mL
- Cell inoculation (ECS) – 2 - 3 x 10^6 cells
- Cell inoculation (Lumen) – 1.5 x 10^6 cells
- ECS sampling port – 2
- Electrodes embedded in the cartridge - 4

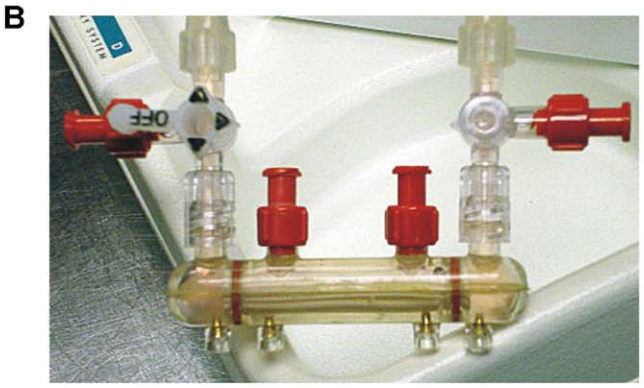

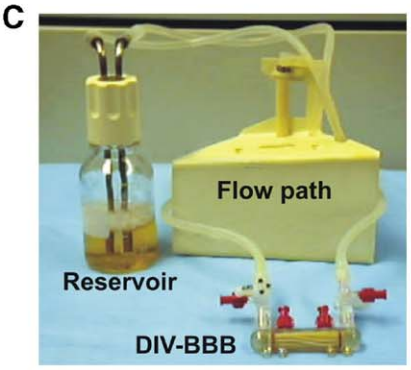

Fig. 5 – Diagrammatic representation of the hollow fiber cartridge system and the computer-controlled TEER monitoring device. (A) three-dimensional representation of DIV-BBB. Note the electrodes embedded in the lower half of the scaffold. Detailed dimensional and functional characteristics are given in the table. (B) picture showing the DIV-BBB in use. A bundle of porous polypropylene hollow fibers is suspended in the chamber. The two three-way stopcocks on either side regulate the access to the luminal compartment. (C) a fully assembled DIV-BBB with flow path and medium reservoir. The hollow fibers are in continuity with the medium source (bottle) through a flow path consisting of gas-permeable silicon tubing. (D) The TEER measurement system (Flocel Inc.) allows for computer controlled monitoring of the BBB in real time. This newly developed platform interface allows for the monitoring of BBB integrity during the experiments. TEER can also be used to assess for BBB formation during preliminary steps. See text for details.

trans-capillary pore size of 0.64 μm inside a polycarbonate-sealed chamber (volume of extraluminal space (ECS) = 1.15 cm^3, extraluminal surface area = 1.19 cm^2). The porosity of the hollow fibers allows gas and nutrient exchange between the two compartments (luminal/extraluminal) but does not permit cells to pass. Both luminal and abluminal areas are accessible

Table 1 – Advantages of DIV-BBB

1. Glucose, oxygen, flow (shear), and temperature can be independently varied
2. Continuous monitoring of BBB integrity (TEER)
3. Variable levels of Shear stress can be applied.
4. Administration of Biological agents into intra- or extraluminal compartment
5. Easy separation of EC from astrocytes for analysis
6. Cultures remain viable for extended period (several months)
7. Easy determination of the role of individual variables modulating BBB function
8. DIV-BBB is not limited to BBB cells

by ports in the circuit connected with a medium reservoir and a pulsatile pump apparatus. Four electrodes are embedded in the bottom of each cartridge (Fig. 5B) allowing for faster and more accurate TEER measurements by real-time computerized monitoring systems. Gaseous exchange occurs while media flows (≈25 mL) through gas permeable silicone tubing that connects the cartridge and the medium reservoir (Fig. 5C). The pump (CellMax® QUAD Artificial Capillary Cell Culture System, Spectrum Laboratories CA) is capable of generating flow rates of 1–50 mL/min corresponding to shear stress levels of approximately 1–200 dyn/cm^2. In order to allow for cell adhesion, we used an initial flow rate of 1 mL/min for the first 48 h following cell inoculation and then adjusted the flow to 4 mL/min (i.e., 4 dyn/cm^2). Both compartmental surfaces were coated with 3 μg/cm^2 fibronectin and the extraluminal capillary side was precoated with poly-D-lysine (3 μg/cm^2) as well. The entire apparatus resided in a water-jacketed incubator with 5% CO_2 at 37 °C. For sterile sampling, it could be moved into a laminar flow hood. BAEC were seeded intraluminally and allowed to establish themselves for 7–15 days with or without extraluminal C6. The amount of cells seeded was ≈1.5×10^6 BAEC and ≈2×10^6 C6.

4.3. *Cell metabolism: lactate production and glucose consumption*

In conjunction with TEER monitoring, indicators of cell metabolism were used to monitor cell expansion in both the DIV-BBB and Transwell apparatus. Depletion of the main carbohydrate component of the growth medium (glucose) and accumulation of metabolically produced lactic acid are used as indicators of cell growth (Stanness et al., 1996, 1997, 1999; Cucullo et al., 2002; Ballermann and Ott, 1995; Deli et al., 2005; McAllister et al., 2001). For this purpose, luminal and extracapillary space were sampled at daily intervals. The calculations for glucose consumption (mg/day) and lactate production rates (mg/day) are based on medium replacement, volume of non-replaced medium and previous values. Glucose consumption rate was calculated based on the concentration of glucose in fresh and unreplaced medium in the system, according to the following equation:

$$\frac{(V_n \times G_n) + (V_o \times G_p) - (V_{\text{total}} \times G_c)}{T_c - T_p}, \quad (1)$$

where V represents added volumes of medium (mL), G is the glucose concentration (mg/mL), T is time of sampling (in fractions of days), c and P indicate the current and previous samples, respectively, n represents (new) fresh medium added after previous sampling, whereas o represents old, unreplaced medium. Lactate production rate was calculated similarly:

$$\frac{(V_t \times L_c) - (V_n \times L_n) + (V_u \times L_p)}{T_c - T_p}, \quad (2)$$

where L refers to the concentration of lactic acid in mg/mL. A dual-channel immobilized oxidase enzyme biochemistry (YSI 2700 SELECT, YSI Inc., Yellow Springs, Ohio) was used to measure lactate and glucose in the cell culture medium. Data obtained with the described equation were then converted in mmol/day.

4.4. *DIV-BBB TEER measurement system*

The trans-endothelial electrical resistance (TEER) measurement provides a quick and easy evaluation of the integrity of the blood–brain barrier model. We used a newly developed TEER measurement device (Flocel Inc., Cleveland, Ohio), which utilizes electronic multiplexing to measure multiple cartridges in quick succession and assess the integrity and viability of tissue culture models rapidly and reliably (Fig. 5D). The device uses a universal serial bus (USB) interface to a PC computer. To sample, the excitation voltage is applied across the excitation electrodes inserted in each cartridge and the microcontroller computes the resistivity and capacitance per cm^2 of the barrier from physical parameters. TEER was measured continuously from the initial setup throughout the course of each experiment.

4.5. *Transwell systems*

Cells were co-cultured using sets of 12-well Transwell-Clear Polyester Membrane apparatus (Costar cat. #3460) that feature a vertical side by side diffusion system through a thin, microscopically transparent polyester membrane of 12 mm diameter and 0.4 μm pore size mounted on a double chamber (Fig. 6). BAEC were seeded on the top side of the membrane and allowed to establish themselves for 3 days. C6 were then seeded on the underside of the filter (co-cultures only). The amount of cells ranged from 1×10^5 (BAEC) to 1.5×10^5 (C6). TEER was monitored every 2 days beginning at "day 1" of co-culture. The equipment consisted of a tissue resistance measurement chamber (Endohm chamber, WPI) that provides a reproducible electrical resistance measurement of endothelial tissue culture cups. In conjunction with TEER monitoring, BAEC monolayer integrity was also assessed by inspection with phase contrast microscopy.

4.6. *Drug permeability: uptake of [^{14}C]phenytoin and [^{3}H] sucrose*

A concentrated bolus of [^{14}C] phenytoin and [^{3}H] sucrose was injected into the lumen and the diffusion into the extracapillary space was monitored over time while maintaining a 1 mL/min intraluminal perfusion rate. Samples were taken from ECS or the lumen as previously described (Stanness et al., 1997; Salvetti et al., 2002), at time 0 (immediately after the injection) and at 1, 3, 5, 10, 15, 30, and 60 min following the injection. Samples removed from ECS were replaced with equal volumes of medium. 100 μL

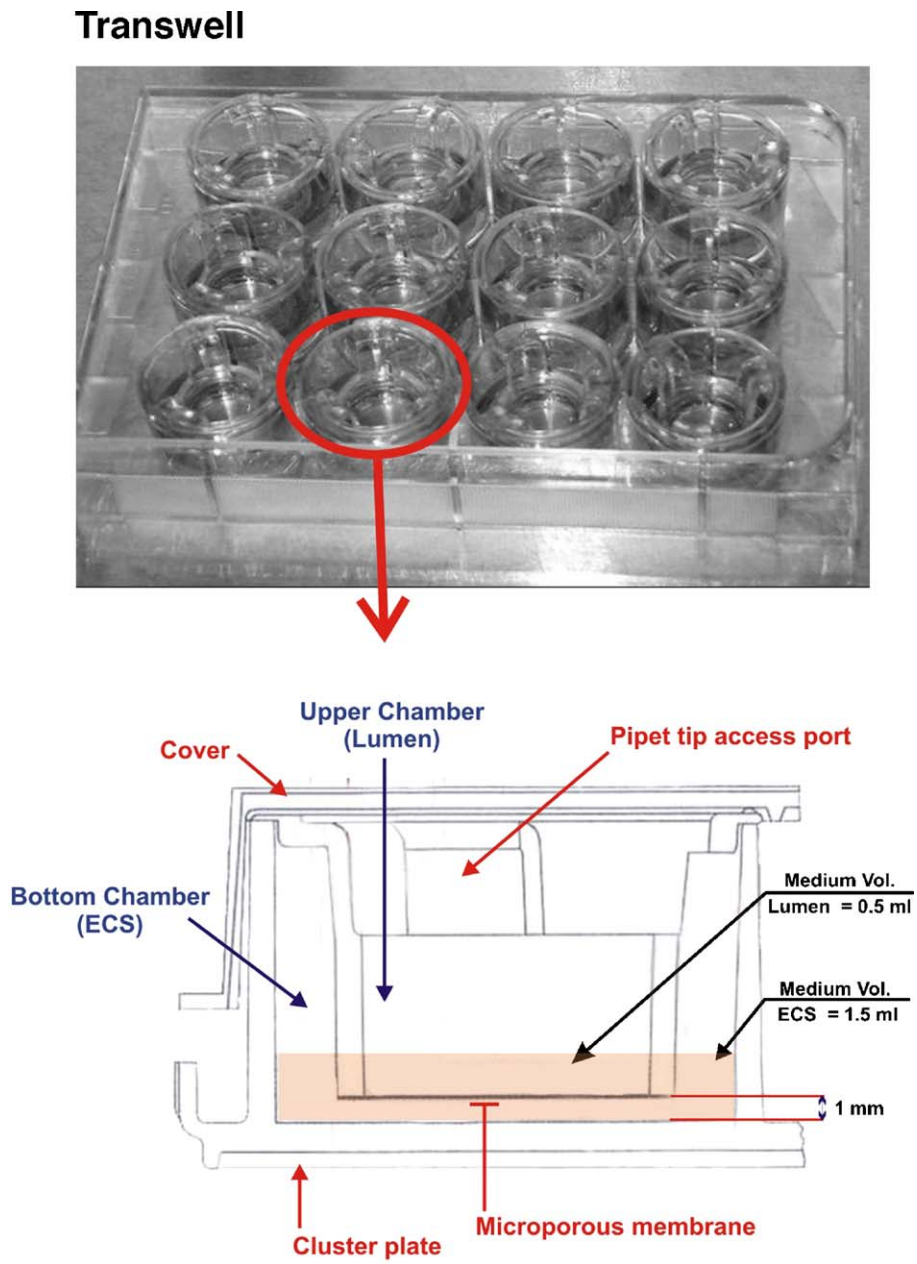

Fig. 6 – Schematic representation of a typical Transwell apparatus. The Transwell system consists of cultured BAEC monolayers grown on microporous membranes. Cultured C6 glial cells were seeded on the underside of the membrane and release soluble factors, which preserve some of the BBB properties. This system allows for study of bidirectional transport across the BBB. See text for more details.

samples of [^{3}H] sucrose or [^{14}C] phenytoin were introduced into vials with 4 mL of Ready Protein Beckman scintillation cocktail (Packard Ultima Gold, ECN, Costa Mesa, CA, USA).

Radioactivity was counted with an LS 6500 scintillation counter (Beckman). Permeability was calculated by graphical integration of drug concentration in the lumen and in ECS over 60 min. Permeability for a given compound was calculated by integrating the area under the ECS and lumen data points according to the following formula:

$$K = \frac{C_{ECS}(t) - C_{ECS}(0)}{[AUC_{lumen}]_0^t - [AUC_{ECS}]_0^t},$$

where K is a constant used to normalize rate of flux for the luminal surface and lumen/ECS volume ratios; C_{ECS} (t) and C_{ECS} (0) are the extraluminal space concentrations of compound x at time (t) and time zero as previously reported (Stanness et al., 1997; Salvetti et al., 2002). A similar procedure was used to assess drug permeability in the Transwell system. Note also that the luminal and extraluminal compartments of Transwell apparatus used in our study were similar in volume and surface areas to the DIV-BBB model, but the volume of circulating medium in the DIV-BBB was far greater (≈25 mL) than the donor volume (upper chamber) in the Transwell (0.5 mL).

4.7. *BBB opening by hyperosmolar mannitol*

Infusion of 10 mL of growth medium containing mannitol at a concentration of 1.6 M was used to open the BBB (Rapoport, 2000). The solution was prepared under sterile conditions and injected intraluminally at a perfusion rate of 1 mL/min. TEER was monitored during the course of the experiment to assess BBB failure and recovery. A concentrated bolus containing both [^{14}C] phenytoin and [^{3}H] sucrose was injected into the lumen 1 min following mannitol perfusion and flux into the extracapillary space was monitored over time as previously described. In the Transwell system, the regular luminal media ware replaced with one containing mannitol at the final concentration of 1.6 M and left in the luminal chamber for 10 min in order to reproduce experimental parameters similar to the one established in the DIV-BBB. The medium in the luminal chamber was then removed and replaced with fresh one containing [^{14}C] phenytoin and [^{3}H] sucrose at similar concentrations to those tested in the DIV-BBB. Note that in the DIV-BBB apparatus the intraluminal flow removes the mannitol from the luminal chamber (the mannitol is then exhausted in the reservoir), lack of flow in the Transwell system required manual removal of the mannitol solution.

Acknowledgments

This work was supported by Philip Morris USA and Philip Morris International external research award to Luca Cucullo and NIH-2RO1 HL51614, NIH-RO1 NS43284 NIH-RO1 NS38195 to Damir Janigro.

REFERENCES

Abbott, N.J., 2002. Astrocyte–endothelial interactions and blood–brain barrier permeability. J. Anat. 200, 629–638.

Abbott, N.J., 2005. Dynamics of CNS barriers: evolution, differentiation, and modulation. Cell. Mol. Neurobiol. 25, 5–23.

Akimoto, S., Mitsumata, M., Sasaguri, T., Yoshida, Y., 2000. Laminar shear stress inhibits vascular endothelial cell proliferation by inducing cyclin-dependent kinase inhibitor p21(Sdi1/Cip1/Waf1). Circ. Res. 86, 185–190.

Ando, J., Kamiya, A., 1996. Flow-dependent regulation of gene expression in vascular endothelial cells. Jpn. Heart J. 37, 19–32.

Ballermann, B.J., Ott, M.J., 1995. Adhesion and differentiation of endothelial cells by exposure to chronic shear stress: a vascular graft model. Blood Purif. 13, 125–134.

Ballermann, B.J., Dardik, A., Eng, E., Liu, A., 1998. Shear stress and the endothelium. Kidney Inter., Suppl. 67, S100–S108.

Banks, W.A., 2005. Blood–brain barrier transport of cytokines: a mechanism for neuropathology. Curr. Pharm. Des 11, 973–984.

Boveri, M., Berezowski, V., Price, A., Slupek, S., Lenfant, A.M., Benaud, C., Hartung, T., Cecchelli, R., Prieto, P., Dehouck, M.P., 2005. Induction of blood–brain barrier properties in cultured brain capillary endothelial cells: comparison between primary glial cells and C6 cell line. Glia 51, 187–198.

Brooks, A.R., Lelkes, P.I., Rubanyi, G.M., 2004. Gene expression profiling of vascular endothelial cells exposed to fluid mechanical forces: relevance for focal susceptibility to atherosclerosis. Endothelium 11, 45–57.

Brown, R.C., Davis, T.P., 2005. Hypoxia/aglycemia alters expression of occludin and actin in brain endothelial cells. Biochem. Biophys. Res. Commun. 327, 1114–1123.

Brown, R.C., Egleton, R.D., Davis, T.P., 2004. Mannitol opening of the blood–brain barrier: regional variation in the permeability of sucrose, but not 86Rb+ or albumin. Brain Res. 1014, 221–227.

Cucullo, L., McAllister, M.S., Kight, K., Krizanac-Bengez, L., Marroni, M., Mayberg, M.R., Stanness, K.A., Janigro, D., 2002. A new dynamic *in vitro* model for the multidimensional study of astrocyte-endothelial cell interactions at the blood–brain barrier. Brain Res. 951, 243–254.

Cucullo, L., Aumayr, B., Rapp, E., Janigro, D., 2005. Drug delivery and *in vitro* models of the blood–brain barrier. Curr. Opin. Drug Discov. Dev. 8, 89–99.

De Boer, A.B., De Lange, E.L., Van der Sandt, I.C., Breimer, D.D., 1998. Transporters and the blood–brain barrier (BBB). Int. J. Clin. Pharmacol. Ther. 36, 14–15.

Deli, M.A., Abraham, C.S., Kataoka, Y., Niwa, M., 2005. Permeability studies on *in vitro* blood–brain barrier models: physiology, pathology, and pharmacology. Cell. Mol. Neurobiol. 25, 59–127.

Desai, S.Y., Marroni, M., Cucullo, L., Krizanac-Bengez, L., Mayberg, M.R., Hossain, M.T., Grant, G.G., Janigro, D., 2002. Mechanisms of endothelial survival under shear stress. Endothelium 9, 89–102.

Ellison, J.A., Barone, F.C., Feuerstein, G.Z., 1999. Matrix remodeling after stroke. De novo expression of matrix proteins and integrin receptors. Ann. N. Y. Acad. Sci. 890, 204–222.

Emmi, A., Wenzel, H.J., Schwartzkroin, P.A., Taglialatela, M., Castaldo, P., Bianchi, L., Nerbonne, J., Robertson, G.A., Janigro, D., 2000. Do glia have heart? Expression and functional role for ether-a-go-go currents in hippocampal astrocytes. J. Neurosci. 20, 3915–3925.

Fortin, D., Salame, J.A., Desjardins, A., Benko, A., 2004. Technical modification in the intracarotid chemotherapy and osmotic blood–brain barrier disruption procedure to prevent the relapse of carboplatin-induced orbital pseudotumor. AJNR Am. J. Neuroradiol. 25, 830–834.

Grant, G.A., Abbott, N.J., Janigro, D., 1998. Understanding the physiology of the blood–brain barrier: in vitro models. News Physiol. Sci. 13, 287–293.

Hagenbuch, B., Gao, B., Meier, P.J., 2002. Transport of xenobiotics across the blood–brain barrier. News Physiol. Sci. 17, 231–234.

Hamm, S., Dehouck, B., Kraus, J., Wolburg-Buchholz, K., Wolburg, H., Risau, W., Cecchelli, R., Engelhardt, B., Dehouck, M.P., 2004. Astrocyte mediated modulation of blood–brain barrier permeability does not correlate with a loss of tight junction proteins from the cellular contacts. Cell Tissue Res. 315, 157–166.

Hawkins, B.T., Davis, T.P., 2005. The blood–brain barrier/neurovascular unit in health and disease. Pharmacol. Rev. 57, 173–185.

Hawkins, B.T., Egleton, R.D., 2006. Fluorescence imaging of blood–brain barrier disruption. J. Neurosci. Methods 151 (2), 262–267.

Heo, J.H., Han, S.W., Lee, S.K., 2005. Free radicals as triggers of brain edema formation after stroke. Free Radical Biol. Med. 39, 51–70.

Hori, S., Ohtsuki, S., Tachikawa, M., Kimura, N., Kondo, T., Watanabe, M., Nakashima, E., Terasaki, T., 2004. Functional expression of rat ABCG2 on the luminal side of brain capillaries and its enhancement by astrocyte-derived soluble factor(s). J. Neurochem. 90, 526–536.

Janigro, D., Leaman, S.M., Stanness, K.A., 1999. Dynamic modeling of the blood–brain barrier: a novel tool for studies of drug delivery to the brain. Pharm. Sci. Technol. Today 2, 7–12.

Korn, A., Golan, H., Melamed, I., Pascual-Marqui, R., Friedman, A., 2005. Focal cortical dysfunction and blood–brain barrier

disruption in patients with postconcussion syndrome. J. Clin. Neurophysiol. 22, 1–9.
Kramer, S.D., Schutz, Y.B., Wunderli-Allenspach, H., Abbott, N.J., Begley, D.J., 2002. Lipids in blood–brain barrier models *in vitro*: II. Influence of glial cells on lipid classes and lipid fatty acids. In Vitro Cell Dev. Biol., Anim. 38, 566–571.
Krizanac-Bengez, L., Kapural, M., Parkinson, F., Cucullo, L., Hossain, M., Mayberg, M.R., Janigro, D., 2003. Effects of transient loss of shear stress on blood–brain barrier endothelium: role of nitric oxide and IL-6. Brain Res. 977, 239–246.
Krizanac-Bengez, L., Mayberg, M.R., Janigro, D., 2004. The cerebral vasculature as a therapeutic target for neurological disorders and the role of shear stress in vascular homeostatis and pathophysiology. Neurol. Res. 26, 846–853.
Krizanac-Bengez, L., Mayberg, M.R., Cunningham, E., Hossain, M., Ponnampalam, S., Parkinson, F.E., Janigro, D., 2006. Loss of shear stress induces leukocyte-mediated cytokine release and blood–brain barrier failure in dynamic *in vitro* blood–brain barrier model. J. Cell. Physiol. 206 (1), 68–77.
Laterra, J., Goldstein, G.W., 1991. Astroglial-induced *in vitro* angiogenesis: requirements for RNA and protein synthesis. J. Neurochem. 57, 1231–1239.
Lauer, R., Bauer, R., Linz, B., Pittner, F., Peschek, G.A., Ecker, G., Friedl, P., Noe, C.R., 2004. Development of an *in vitro* blood–brain barrier model based on immortalized porcine brain microvascular endothelial cells. Farmaco 59, 133–137.
Liberto, C.M., Albrecht, P.J., Herx, L.M., Yong, V.W., Levison, S.W., 2004. Pro-regenerative properties of cytokine-activated astrocytes. J. Neurochem. 89, 1092–1100.
Lin, K., Hsu, P.P., Chen, B.P., Yuan, S., Usami, S., Shyy, J.Y., Li, Y.S., Chien, S., 2000. Molecular mechanism of endothelial growth arrest by laminar shear stress. Proc. Natl. Acad. Sci. U. S. A. 97, 9385–9389.
McAllister, M.S., Krizanac-Bengez, L., Macchia, F., Naftalin, R.J., Pedley, K.C., Mayberg, M.R., Marroni, M., Leaman, S., Stanness, K.A., Janigro, D., 2001. Mechanisms of glucose transport at the blood–brain barrier: an *in vitro* study. Brain Res. 904, 20–30.
Minakawa, T., Bready, J., Berliner, J., Fisher, M., Cancilla, P.A., 1991. *In vitro* interaction of astrocytes and pericytes with capillary-like structures of brain microvessel endothelium. Lab. Invest. 65, 32–40.
Mizuguchi, H., Utoguchi, N., Mayumi, T., 1997. Preparation of glial extracellular matrix: a novel method to analyze glial–endothelial cell interaction. Brain Res. Brain Res. Protoc. 1, 339–343.
Ott, M.J., Ballermann, B.J., 1995. Shear stress-conditioned, endothelial cell-seeded vascular grafts: improved cell adherence in response to *in vitro* shear stress. Surgery 117, 334–339.
Pekny, M., Stanness, K.A., Eliasson, C., Betsholtz, C., Janigro, D., 1998. Impaired induction of blood–brain barrier properties in aortic endothelial cells by astrocytes from GFAP-deficient mice. Glia 22, 390–400.
Rapoport, S.I., 2000. Osmotic opening of the blood–brain barrier: principles, mechanism, and therapeutic applications. Cell. Mol. Neurobiol. 20, 217–230.
Salvetti, F., Cecchetti, P., Janigro, D., Lucacchini, A., Benzi, L., Martini, C., 2002. Insulin permeability across an *in vitro* dynamic model of endothelium. Pharm. Res. 19, 445–450.
Shusta, E.V., 2005. Blood–brain barrier genomics, proteomics, and new transporter discovery. NeuroRx 2, 151–161.
Siegal, T., Rubinstein, R., Bokstein, F., Schwartz, A., Lossos, A., Shalom, E., Chisin, R., Gomori, J.M., 2000. *In vivo* assessment of the window of barrier opening after osmotic blood–brain barrier disruption in humans. J. Neurosurg. 92, 599–605.
Sobue, K., Yamamoto, N., Yoneda, K., Hodgson, M.E., Yamashiro, K., Tsuruoka, N., Tsuda, T., Katsuya, H., Miura, Y., Asai, K., Kato, T., 1999. Induction of blood–brain barrier properties in immortalized bovine brain endothelial cells by astrocytic factors. Neurosci. Res. 35, 155–164.
Stanness, K.A., Guatteo, E., Janigro, D., 1996. A dynamic model of the blood–brain barrier "in vitro". Neurotoxicology 17, 481–496.
Stanness, K.A., Westrum, L.E., Fornaciari, E., Mascagni, P., Nelson, J.A., Stenglein, S.G., Myers, T., Janigro, D., 1997. Morphological and functional characterization of an *in vitro* blood–brain barrier model. Brain Res. 771, 329–342.
Stanness, K.A., Neumaier, J.F., Sexton, T.J., Grant, G.A., Emmi, A., Maris, D.O., Janigro, D., 1999. A new model of the blood–brain barrier: co-culture of neuronal, endothelial and glial cells under dynamic conditions. NeuroReport 10, 3725–3731.
Toborek, M., Lee, Y.W., Flora, G., Pu, H., Andras, I.E., Wylegala, E., Hennig, B., Nath, A., 2005. Mechanisms of the blood–brain barrier disruption in HIV-1 infection. Cell. Mol. Neurobiol. 25, 181–199.
van Vulpen, M., Kal, H.B., Taphoorn, M.J., El Sharouni, S.Y., 2002. Changes in blood–brain barrier permeability induced by radiotherapy: implications for timing of chemotherapy? (Review). Oncol. Rep. 9, 683–688.
Wasserman, S.M., Topper, J.N., 2004. Adaptation of the endothelium to fluid flow: *in vitro* analyses of gene expression and *in vivo* implications. Vasc. Med. 9, 35–45.
Ziegler, T., Nerem, R.M., 1994. Effect of flow on the process of endothelial cell division. Arterioscler. Thromb. 14, 636–643.